

## High Performance Woven Mesh Heat Exchangers

Richard A. Wirtz, Chen Li, Ji-Wook Park and Jun Xu  
 Mechanical Engineering Department/MS 312  
 University of Nevada, Reno  
 Reno, NV 89557

### ABSTRACT

Simple-to-fabricate woven mesh structures, consisting of bonded laminates of two-dimensional plain-weave conductive screens, or three-dimensional orthogonal weaves are described. Geometric equations show that these porous matrices can be fabricated to have a wide range of porosity and a highly anisotropic thermal conductivity vector. A mathematical model of the thermal performance of such a mesh, deployed as a heat exchange surface, is developed. Measurements of pressure drop and overall heat transfer rate are reported and used with the performance model to develop correlation equations of mesh friction factor and Colburn j-factor as a function of coolant properties, mesh characteristics and flow rate through the mesh. A heat exchanger performance analysis delineates conditions where the two mesh technologies offer superior performance.

$t$  = thickness of mesh  
 $T$  = temperature  
 $U$  = effective conductance of mesh  
 $W$  = width of mesh  
 $\beta$  = heat transfer surface area to volume ratio  
 $\Delta P$  = pressure drop  
 $\varepsilon$  = porosity  
 $\theta$  = mesh angle  
 $\rho$  = fluid density  
 $\mu$  = fluid viscosity

#### Subscripts

$f$  = fluid  
 $i, o$  = inlet, outlet  
 $s$  = solid  
 $x, y, z$  = coordinates

### NOMENCLATURE

$cf$  = compression factor  
 $c$  = fluid specific heat  
 $d$  = wire diameter of mesh  
 $D_h$  = hydraulic diameter of mesh  
 $f$  = friction factor  
 $G$  = fluid mass velocity  
 $h$  = unit surface conductance  
 $H$  = height of mesh  
 $j$  = Colburn j-factor  
 $k$  = thermal conductivity  
 $ke$  = effective thermal conductivity  
 $M$  = mesh number  
 $P$  = pressure  
 $Pr$  = Prandtl number  
 $q$  = heat transfer rate  
 $q''$  = heat flux  
 $r$  =  $dy/dx$   
 $Re$  = Reynolds number  
 $St$  = Stanton number

### INTRODUCTION

Kays and London [1984] have pointed out that a most effective way to increase the performance of a heat exchanger is to increase its surface area to volume ratio,  $\beta$ . Small-particle packed beds and foamed metals are porous materials having large  $\beta$ -values. Unfortunately, due to the tortuosity effect in conjunction with the high porosity ( $\varepsilon$ ) of these materials, their effective thermal conductivity ( $ke$ ) is relatively small so that much of the gain in performance obtained by having a large  $\beta$  is lost by having a relatively small  $ke$ . Typical values of effective thermal conductivity in fused-particle packed beds are 10% - 15% of the particle thermal conductivity. Commercially available metal foam such as aluminum foam has an effective thermal conductivity that ranges from only 2% to 6% of the base metal value [Calmidi and Mahajan, 1999].

An anisotropic porous matrix having a large specific surface area and a large effective thermal conductivity in a particular direction will result in a very effective heat exchange surface. A woven mesh of heat conducting filaments can be configured to have these

## Report Documentation Page

<b>Report Date</b> 29JUL2002	<b>Report Type</b> N/A	<b>Dates Covered (from... to)</b> -
<b>Title and Subtitle</b> High Performance Woven Mesh Heat Exchangers	<b>Contract Number</b>	
	<b>Grant Number</b>	
	<b>Program Element Number</b>	
<b>Author(s)</b>	<b>Project Number</b>	
	<b>Task Number</b>	
	<b>Work Unit Number</b>	
<b>Performing Organization Name(s) and Address(es)</b> Mechanical Engineering Department/MS 312 University of Nevada, Reno Reno, NV 89557	<b>Performing Organization Report Number</b>	
<b>Sponsoring/Monitoring Agency Name(s) and Address(es)</b>	<b>Sponsor/Monitor's Acronym(s)</b>	
	<b>Sponsor/Monitor's Report Number(s)</b>	
<b>Distribution/Availability Statement</b> Approved for public release, distribution unlimited		
<b>Supplementary Notes</b> See Also ADM201460. Papers from Unclassified Proceedings from the 11th Annual AAIA/MDA Technology Conference held in Monterey, CA from 29 Jul - 2 Aug 2002.		
<b>Abstract</b>		
<b>Subject Terms</b>		
<b>Report Classification</b> unclassified	<b>Classification of this page</b> unclassified	
<b>Classification of Abstract</b> unclassified	<b>Limitation of Abstract</b> SAR	
<b>Number of Pages</b> 7		

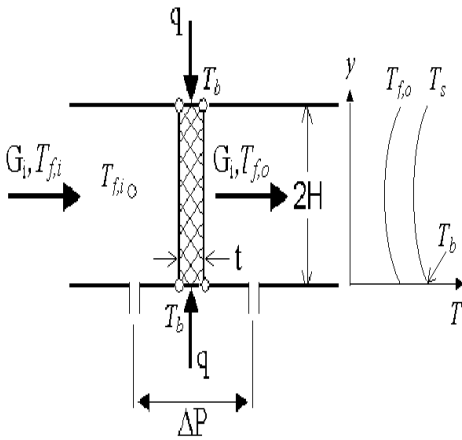


Fig. 1 Heat exchange implementation of a thermally conductive woven mesh.

characteristics. Geometric equations show that these porous matrices can be fabricated to have a wide range of porosity and specific surface area; and a highly anisotropic thermal conductivity vector can be achieved.

These attributes allow for the design of small, high-performance single-fluid parallel-plate heat exchangers that are more universally applicable than conventional heat exchangers because the mesh can readily be made to conform to complex surface contours. Because of the high thermal conductance achieved, exchangers can be designed for applications where spatial temperature uniformity and/or high localized spot cooling are required.

The present work focuses on two woven mesh configurations:

1. Three-dimensional orthogonal weaves that consist of three metallic wire filaments having their axes aligned with the coordinate axes, and
2. Laminates of plain-weave metallic screens stacked to form a three dimensional structure.

The fabrication methodology for each structure is explored. Models of the porosity, specific surface area, effective thermal conductivity and overall thermal performance of the mesh, deployed as a single-fluid heat exchanger, are developed. Measurements are reported for fabricated test articles; and, mesh Stanton number and friction factor correlations are reported.

#### HEAT EXCHANGER IMPLEMENTATION

Figure 1 shows a woven mesh implemented as a heat transfer surface in a parallel plate exchanger. The mesh

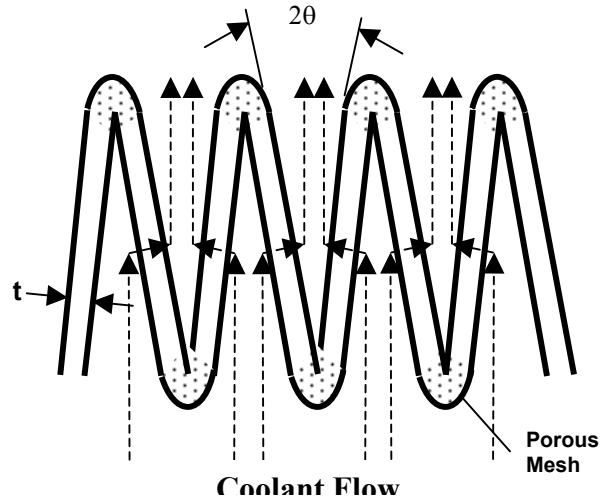


Fig. 2 Plan view of woven mesh serpentine wall. Divergence angle controls uniformity of flow through wall segments.

is shown in edge-view in a channel having half-height  $H$ . The mesh thickness is  $t$ . Heat ( $q$ ) is conducted from the heated plates (at temperature  $T_b$ ) into the mesh, and then by convection to the fluid flowing through the mesh. The mesh wire filament axes are arranged so that the predominant y-filaments are perpendicular to the channel walls so that conduction from the walls is facilitated. Other wire filaments in thermal contact with the predominant filaments act as fins, increasing the specific surface area of the mesh.  $G_i$  and  $T_{fi}$  are the coolant approach mass velocity and temperature, respectively.  $\Delta P$  is the pressure drop across the exchange matrix. The right-hand segment of the figure shows the expected temperature distribution of the woven mesh ( $T_s$ ) and the exit-plane coolant ( $T_{fo}$ ).

Figure 2 shows a plan view of a segment of the coolant passage of a flow-through electronics-cooling module (FTM). These units are essentially parallel plate heat exchangers where electronic components that are mounted on the plate outer surfaces are cooled by the passage of a coolant flowing between the plates. Fin stock normally found between the plates can be replaced with a woven-mesh porous wall that is laid out in a serpentine pattern. Mesh wire filaments are oriented between the side plates of the FTM as in Fig. 1. The woven-mesh porous wall segment so formed is shown in plan view, and typical flow paths for some fluid elements are shown. This configuration results in a relatively low coolant pressure drop since fluid parcel paths through the mesh are short, and the serpentine mesh layout results in a large face area leading to low superficial mass velocities of coolant through the mesh. The divergence/convergence angle of wall segments,  $2\theta$  controls the flow uniformity through each segment. Heat transfer is by conduction through the module side

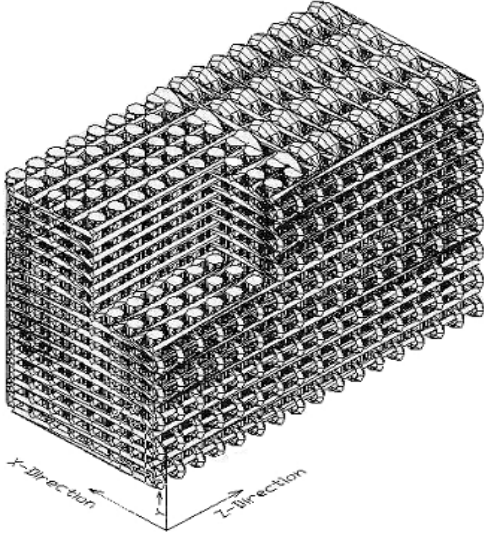


Fig. 3 Three-dimensional orthogonal "stacked" weave.

plates, and then by conduction and convection within the (porous) woven mesh.

**3D Woven-Mesh Geometry.** Figure 3 shows a three-dimensional orthogonal stacked-weave that consists of three separate wire filaments of diameters  $d_x$ ,  $d_y$  and  $d_z$ , having axes aligned with the coordinates,  $x$ ,  $y$  and  $z$ , respectively. We require that wire filaments touch at all possible filament intersections so that filaments can be bonded to facilitate conduction within the mesh. This establishes the wire pitch in each coordinate direction. Coolant flow is presumed to be primarily in the  $x$ - $z$  plane. The  $y$ -wire filament diameter,  $d_y$  is larger than  $d_x$  and  $d_z$  so that the effective thermal conductivity in the  $y$ -direction,  $ke_y$  is larger than  $ke_x$  or  $ke_z$ . In this way, heat is transferred to the fluid by conduction primarily along the  $y$ -filaments; then to the  $x$ - and  $z$ -filaments, which act as fins. We also require that  $d_x = d_z$ ; and we define  $r = d_y/d_z$  as the diameter ratio. We designate the three-dimensional orthogonal weave shown in fig. 1 a "stacked weave" since there is no interweaving of wire filaments in any of the three principal planes. This approach allows for a very dense structure.

**Screen-laminate Geometry.** Figure 4 shows two-dimensional plain-weave screens stacked together to form a screen laminate. Each screen has woven wires of diameter  $d_y$  and  $d_z$ , with axis parallel to the  $y$ - and  $z$ -axis, respectively. Wire spacing is designated by the mesh numbers,  $M_y$  and  $M_z$ . The laminate has thickness,  $t = cf \cdot n(d_y + d_z)$ , where  $n$  is the number of screen layers of the lamination, and  $cf$  is the compression factor.  $cf$  accounts for interleaving of wire filaments of adjacent screens, and wire crimping at wire intersections. Wire filaments are bonded at intersections to facilitate conduction; and, successive screen layers are bonded together to add rigidity to the structure.

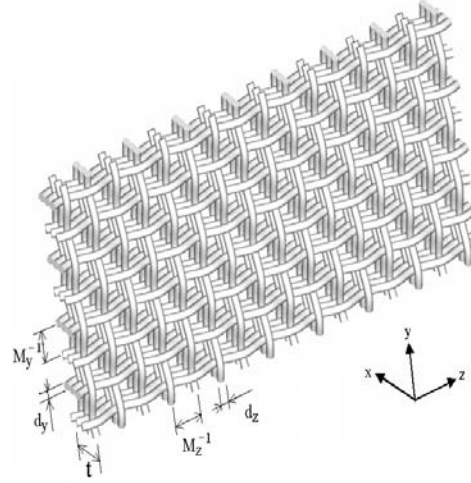


Fig. 4 Screen laminate geometry.

Successive screens can be arranged "in-line" as shown in Figure 4, or in "staggered" configuration, where alternate screen layers are offset in the  $y$  and  $z$  directions by  $0.5 M^l$ . Screen laminates having  $d_y = d_z$  and  $M_y = M_z$  are designated isotropic. If the angle between wire filament axes (the weave angle) is  $90^\circ$ , the screen is an orthogonal weave.

### THEORETICAL CONSIDERATIONS

**Thermal Performance Mode.** The mesh acts as a porous wall of porosity,  $\epsilon$  and thickness,  $t$ . The heat transfer rate is given by

$$q = U(tW)[T_b - T_{f,i}] \quad (1)$$

where  $U$  is the effective conductance of the porous wall and  $(tW)$  is the base area. The porous wall effective conductance can be related to the thermal and physical characteristics of the woven structure. The fluid flow path length through the porous wall is short and flow rates are relatively high, so local thermal equilibrium between the fluid and solid phases is probably not achieved; a two energy equation model is called for. Park et al. [2002] assume that the solid phase temperature is only a function of  $y$ ; and, Newton's cooling law characterizes the local heat flux between the fluid and solid phases

$$q_c'' = \bar{h}[T_s(y) - T_f(x, y)] \quad (2)$$

where  $\bar{h}$  is the mesh heat transfer coefficient (a global average) and  $T_s$  and  $T_f$  are the local mesh and fluid temperatures. Eq. (2) couples the solid and fluid phase energy equations. The porous wall conductance can

then be related to the thermal and physical characteristics of the woven structure as follows:

$$\frac{U \cdot H}{ke_y} = mH \cdot \tanh(mH) \quad (3)$$

where

$$mH = \sqrt{\hat{G}_i (1 - e^{-ntu})} \quad (4)$$

$\hat{G}_i = \frac{cG_i H^2}{ke_y t}$  is a dimensionless coolant superficial mass velocity and  $ntu = St \cdot \frac{\beta t}{\varepsilon}$  is the number of transfer units of the mesh.  $St$  is the mesh Stanton number,  $St = \bar{h} / c_p G$ , where  $G = G_i / \varepsilon$  is the internal flow mass velocity. Equations (3) and (4) show that

$$U \approx \sqrt{\beta ke_y h} \cdot F(ntu) \quad (5)$$

where, for the current application,  $F(ntu) \approx O(1)$ . Therefore, thermal performance is maximized by increasing the specific surface area ( $\beta$ ), the effective thermal conductivity ( $ke_y$ ), and the mesh heat transfer coefficient ( $\bar{h}$ ).

#### THERMAL/FLUID CHARACTERIZATION

*Porosity, Specific Surface Area, Effective Thermal Conductivity Relations.* Xu and Wirtz [2002] and Wirtz et al. [2002] develop models for the porosity, specific surface area and effective thermal conductivity of orthogonal plain-weave screen laminates and orthogonal 3-D weaves, respectively. Figure 5 compares  $\beta d_y$  of the 3D stacked weave and screen laminates with a bed of fused spheres and metal foams. The specific surface area is plotted versus the metal fraction ( $1-\varepsilon$ ). The parameter  $r$  in the figure is the wire filament diameter ratio  $d_y/d_z$ . The figure shows that 3-D stacked weaves with  $r \geq 1$  can be configured to have metal fraction ranging from  $0.589$  to  $\pi/4$  while  $2.36 \leq \beta d_y \leq 2\pi$ .

The theoretical porosity of a packed bed of unconsolidated spheres depends on the packing arrangement [Kaviany, 1995]. It can range from  $\varepsilon = 0.26$  for face centered cubic packing to  $\varepsilon = 0.476$  for simple cubic. However, the *achievable* porosity of a packed bed is difficult to control. A typical porosity for an unconsolidated bed will range from  $0.37$  to  $0.41$ . As a consequence, the metal fraction can range from

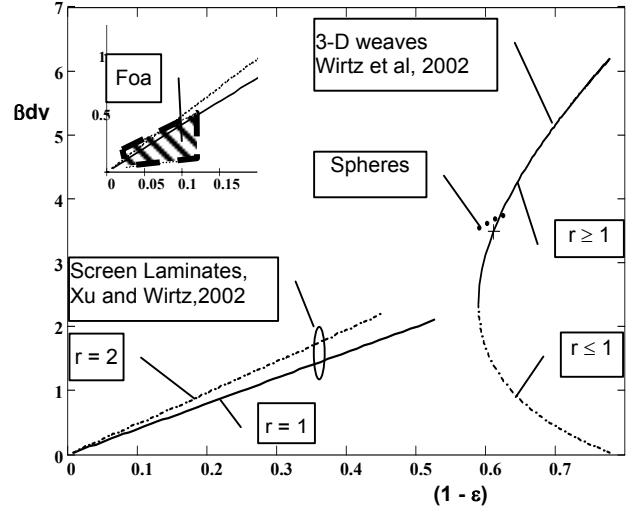


Fig. 5 Specific surface area vs. metal fraction of porous materials.

approximately  $0.59$  to  $0.63$  and  $\beta d_y$  will then range from  $3.54$  to  $3.78$ . A cross designates the 3D weave design point,  $\{r = 2, (1-\varepsilon) = 0.61, \beta d_y = 3.49\}$ . The figure shows that this design point will have a porosity and specific surface area roughly equivalent to that of an unconsolidated bed of spheres. Larger diameter ratios,  $r$  will result in larger achievable specific surface areas.

Xu and Wirtz [2002] show that isotropic plain-weave laminates ( $d_y = d_z$ ,  $M_y = M_z$ ) can be fabricated to have  $0 \leq (1-\varepsilon) \leq 0.534$ . Under these conditions,  $0 \leq \beta d_y \leq 2.13$ . A screen laminate having  $d_y = 2d_z$  ( $r = 2$ ) is also shown. Increasing the predominant wire filament diameter (anisotropic weave) gives rise to a modest increase in specific surface area.

The insert to the figure compares the specific surface area of screen laminates with that achievable with metallic foams [Ashby et al, 2000]. Depending on the origin of the data for foams, screen laminates provide either a significant increase in specific surface area, or they are comparable to the foams. In any case, screen laminates extend the range of metal fraction (or porosity) beyond what appears to be achievable with metal foam.

The combination of screen laminates and 3-D orthogonal weaves allow for the design of high specific surface area heat exchange matrices that span the entire porosity range,  $0.2 \leq \varepsilon \leq 1.0$ . Screen laminated can be configured with  $0 \leq (1-\varepsilon) \leq 0.534$  while the 3D stacked weave is a more dense structure, with metal fraction ranging from  $0.589$  to  $\pi/4$ .

Figure 6 plots the thermal conductivity ratio,  $Ke_y = ke_y/ks$  vs metal fraction for 3-D weaves, screen-laminates, fused spheres and metallic foams ( $ks$  is the base metal thermal conductivity). The figure shows

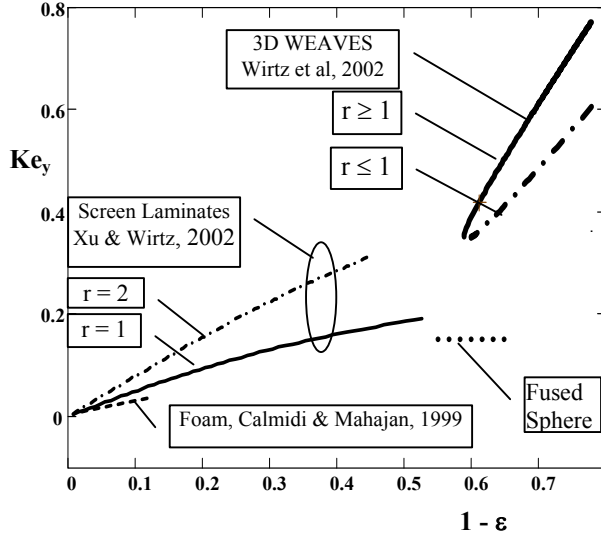


Fig. 6 Effective thermal conductivity of expanded materials.

that for  $r \geq 1$ , the dimensionless effective thermal conductivity of a 3\_D weave can range from 0.351 up to  $\pi/4$  while the metal fraction ranges from 0.589 up to  $\pi/4$ . This is compared to a fused bed of spheres, which is expected to have  $Ke_y(\text{spheres}) \approx 0.15$ . This represents an approximate two- to four-fold increase in thermal performance relative to fused sphere heat transfer matrices (note Eq. 5). Furthermore, incorporation of a third wire filament results in a dramatic increase in the effective thermal conductivity relative to that obtained with isotropic screen-laminate structures, where  $Ke_y$  can range up to 0.2.

The figure also shows the, depending on the screen-laminate configuration, by virtue of their higher effective thermal conductivity, these structures offer a two- to four-fold improvement in performance relative to low-porosity exchange matrices fabricated from metallic foam.

*Woven Mesh Pressure-Drop and Stanton Number Characteristics.* Experiments are performed to measure the pressure drop and porous wall effective conductance,  $U$  of screen laminates [Park et al, 2002] and 3D stacked weaves [Wirtz et al, 2002]. Then, the mesh Stanton number is determined from Eq. (3). Figure 7 compares measured friction factor,

$$f = \frac{\Delta P}{\frac{1}{2} \frac{G^2}{\rho} \beta t} \quad (6)$$

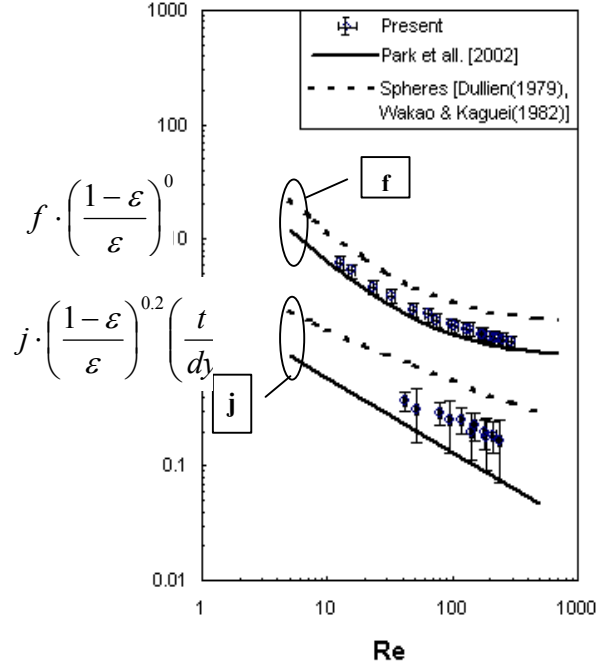


Fig. 7 Modified friction factor and Colburn j-factor.  $\theta = 90^\circ$

and Colburn j-factor,

$$j = St \cdot Pr^{2/3} \quad (7)$$

for the 3D stacked weave [ $r = 2$ ,  $\varepsilon = 0.49$ ] and isotropic plain-weave inline screen-laminates [ $0.53 < \varepsilon < 0.84$ ] with correlations for fused spheres [ $\varepsilon = 0.39$ ]. Woven structures are oriented perpendicular to the superficial mass velocity vector (Fig. 2,  $\theta = 90^\circ$ ). Data are plotted versus the porous media Reynolds number,

$$Re = \frac{GD_h}{\mu} \quad \text{with} \quad D_h = \frac{4\varepsilon}{\beta} \quad \text{the porous media}$$

hydraulic diameter. The figure shows that while fused sphere matrices offer the higher heat transfer coefficient, they also exhibit the highest friction factor. The 3-D weave offers friction factor and heat transfer coefficients intermediate to fused sphere beds and screen laminates. It is interesting to note that, at equal Reynolds number, inline screen laminations offer lower friction factors and higher j-factors than staggered screen laminations.

The woven mesh friction factor correlation for inline laminates is

$$f(\theta, Re) = \left( 0.39 + \frac{0.176}{\tan^2(\theta)} \right) + \left( \frac{24.5}{Re} + \frac{25.863}{Re^{1.16} \cdot \tan(\theta)} \right) \quad (8)$$

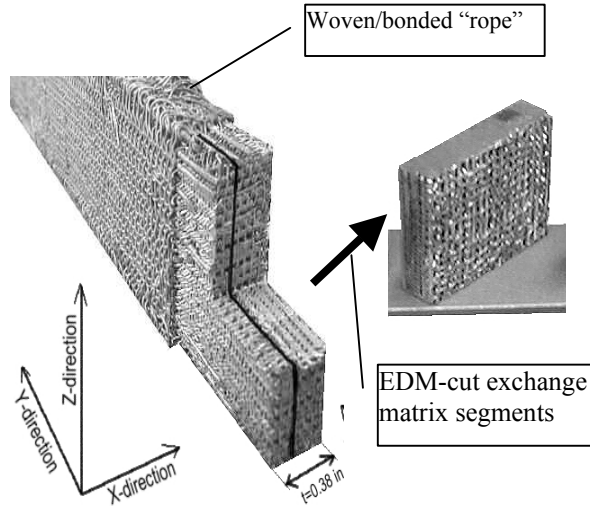


Fig. 8 Three-D woven/bonded mesh fabrication sequence.

Equation (8) illustrates that there are inertial and viscous components to the pressure-drop through the mesh. The inertial component dominates at high Reynolds number whereas the viscous component dominates at  $Re < 10$ . The  $\theta$ -dependent terms represent the increased flow path length through the mesh when  $\theta < 90^\circ$ . The friction factor increases very rapidly as  $\theta \rightarrow 0$ . The Colburn j-factor correlations have power-law forms.

### MESH FABRICATION

Screen laminate fabrication is very straightforward. Commercial grade screen is stacked to form a lamination with the screen elements either aligned or staggered. The wire filaments are then dip-brazed or re-flow soldered to bond the wire filaments at their intersections, and bond adjacent screens together. The resulting structure is very stiff. In fact, there is a commercial stainless steel filter product called Rigimesh®.

Three-D stacked weaves are more challenging. The process, summarized in Fig. 8, involves weaving a wire mesh “rope” of specified wire filament diameters and mesh numbers in the three coordinate directions, braze-bonding the wire filaments at their intersection points, and cutting (via the wire-EDM process) and braze-bonding mesh segments together to form the heat exchange matrix. We have found that failure to maintain a “tight” weave results in a significant increase in the porosity of the mesh, with a consequent reduction in specific surface area and effective thermal conductivity.

Table 1 Mesh characteristics

Characteristic	3D Weave	Screen-Laminate
External Characteristics	$t = 6.35\text{mm}$ , $2H = 25.4\text{mm}$ , $dy = 0.5\text{mm}$ $\varepsilon = 0.39$ , Aluminum, Alloy 1100 Coolant is Air @ 300K ( $Pr = 0.69$ )	
Internal Geometric	$r = 2$ “stacked”	$r = 2$ $Mx = My = 16.1\text{cm}^{-1}$ “in-line” laminate
$\beta [\text{m}^{-1}]$	6781	5921
$Ke_y [\text{W/mK}]$	87.7	82.2
$\Delta P [\text{Pa}]$	Wirtz et al, 2002 correlations	Park et al. 2002 correlations
$h [\text{W/m}^2\text{K}]$		

### MESH PERFORMANCE EVALUATION

Three-dimensional stacked weaves and screen-laminate structures offer considerable design flexibility. Adjustment of the wire diameter ratio,  $r$  (and mesh numbers in the case of screen laminates) allows for control of the structure’s porosity, heat transfer surface area to volume ratio, and effective thermal conductivity. However, the friction factors and Stanton numbers of the heat exchange matrix are comparable to those of other heat transfer surfaces. The question that must be addressed is: under what conditions does either the 3D-weave technology or the 2D screen laminate technology offer superior overall performance.

Recognizing that Park et al. [2002] have shown that screen-laminates can generally be configured to out-perform fused particle systems, in the following we describe a fixed outer geometry comparison [Webb, 1994] of the performance of a 3D-weave exchange matrix with a screen-laminate exchange matrix of the same volume and face area and mass (porosity). The two systems are deployed as in a single-fluid parallel-plate heat exchanger such as a cold-plate or flow-through module.

Table 1 summarizes the characteristics of the two systems. Both exchange matrices are made of aluminum (alloy 1100,  $k_s = 210\text{W/mK}$ ). They have the same thickness (6.35mm) and plate-to-plate spacing ( $2H = 25.4\text{mm}$ ). The coolant is air. The 3D weave is made up of 0.5mm/0.25mm wire ( $r = 2$ ) resulting in an exchange matrix with a porosity of 0.39, specific surface area of  $6781 \text{ m}^{-1}$  and effective thermal conductivity of  $87.7 \text{ W/mK}$ . The screen laminate consists of six layers of orthogonal plain-weave screen made up with 0.5mm/0.25mm wire ( $r = 2$ ) resulting in an exchange matrix with a porosity of 0.39, specific surface area of  $5921 \text{ m}^{-1}$  and effective thermal conductivity of  $82.2 \text{ W/mK}$ .

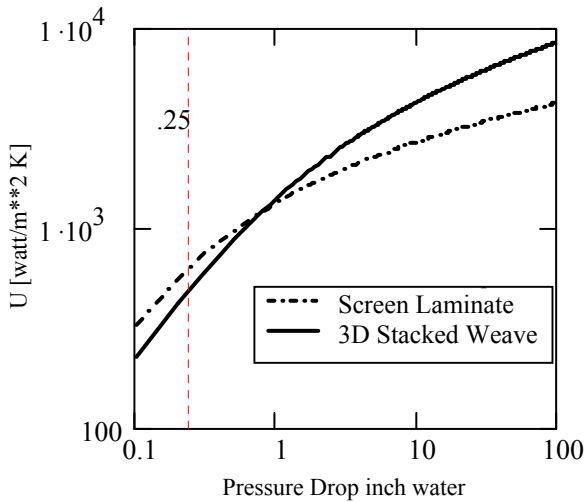


Fig. 9 Screen-laminate / Stacked-weave performance comparison

Figure 9 compares the overall conductance of the two exchanger surfaces as a function of coolant (air) pressure drop across the matrix. The figure shows that, for these conditions, the screen laminate outperforms the 3D stacked weave up to a pressure drop of approximately 250 Pa (1 inch water); then the 3D weave performance is superior. Since the screen laminate offers less flow resistance than the 3D weave, the mass velocity through the array is greater and hence the mesh heat transfer coefficient is greater. This advantage compensates for the lower  $\beta$  and  $Ke$  of the laminate (note eq. (5)). At larger  $\Delta P$ , there is a diminishing return increase in the mesh heat transfer coefficient so that eventually the denser, higher conductivity 3D structure performance becomes dominant. We observe this behavior for other exchanger configurations: at equal coolant pressure drop, the laminate structure dominates at low pressure drops while the 3D structure dominates at high  $\Delta P$ 's.

It should be noted that both of these structures provide equivalent conductance,  $U$  that is generally superior to other more conventional heat transfer surfaces.

### CONCLUSIONS

Woven mesh structures can be configured to have a wide range of  $\beta dy$ -product and porosity. Metallic weaves can be structured to have effective thermal conductivity that is two, or more times greater than what can be achieved with other porous media having equivalent porosity. Mesh heat transfer coefficients and friction factors are comparable to those achieved with other expanded materials. However, high  $\beta$ -values, coupled with high effective thermal conductivity result

in exchange matrices that generally out-perform other exchange matrix configurations.

Screen laminates are generally better suited to applications having limited available pressure of the coolant while the 3D structure is superior in applications that allow for large coolant pressure drop.

Screen laminates are very simple-to-fabricate structures. The 3D woven mesh requires a fairly sophisticated weaving technology.

### ACKNOWLEDGEMENT.

The Missile Defense Agency through the Air Force Office of Scientific Research, USAF, sponsors this work under contract number F49620-99-0286. The views and conclusions contained herein are those of the authors and should not be interpreted as necessarily representing the official policies or endorsements, either expressed or implied, of the Missile Defense Agency, the Air force Office of Scientific Research, or the U.S. Government.

### REFERENCES

- Ashby, M., Evans, A., Fleck, N., Gibson, L., Hutchinson, J., and Wadley, H., *Metal Foams, A Design Guide*, Butterworth Heinemann, 2000.
- Calmidi, V.V. and Mahajan, R.L. (1999) "The Effective Thermal Conductivity of High Porosity Fibrous Metal Foams", *J Heat Transfer*, Vol. 121, pp. 466 - 471
- Kays, W. M. and London, A. L. (1984) *Compact Heat Exchangers*, 3<sup>rd</sup> edn., McGraw-Hill.
- Park, J-W, Ruch, D and Wirtz, R.A. (2002) "Thermal/Fluid Characteristics Of Isotropic Plain-Weave Screen Laminates As Heat Exchange Surfaces", AIAA Paper 2002-0208, AIAA Aerospace Sciences Meeting, Reno, NV, January 2002.
- Wirtz, R. A., Jun Xu, Park, Ji-Wook and Ruch D. Thermal/Fluid Characteristics Of 3\_D Woven Mesh Structures As Heat Exchanger Surfaces, paper no. 1372, Itherm 2002, San Diego, May 2002.
- Xu, J. and Wirtz, R. A., (2002) "In-Plane Effective Thermal Conductivity of Plain-Weave Screen Laminates", *Thermal Challenges in Next Generation Electronic Systems*, Millpress, Rotterdam.